Localization of X-ray Cross Complementing Gene 1 Protein in The Nuclear Matrix is Controlled by Casein Kinase II-dependent Phosphorylation in Response to Oxidative Damage

Yoshiko Kubota[1,*], Takako Takanami[1,2], Atsushi Higashitani[2], and Saburo Horiuchi[1]

[1]Department of Biochemistry, School of Medicine, Iwate Medical University, 19-1 Morioka, Iwate 020-8505, Japan. [2]Laboratory of Genomic Reproductive Biology, Graduate School of Life Sciences, Tohoku University, 2-1-1 Katahira, Aoba-ku, Sendai 980-8577, Japan.

*Address correspondence to: Yoshiko Kubota, PhD, Tel. 81-19-651-5110, Fax. 81-19-653-9244, E-mail: yoshikok@iwate-med.ac.jp

Key words: Base excision repair/single strand break repair, Nuclear foci, Localization

ABSTRACT

Base excision repair/single strand break repair (BER/SSBR) of damaged DNA is a highly efficient process. X-ray cross complementing protein 1 (XRCC1) functions as a key scaffold protein for BER/SSBR factors. Recent work has shown that XRCC1 forms dense foci at sites of DNA damage in a manner dependent on casein kinase II (CK2) phosphorylation. To investigate the mechanism underlying foci formation, we analyzed the subnuclear localization and phosphorylation status of XRCC1 during the repair process by biochemical fractionation of HeLa cellular proteins. The localization was also verified by *in situ* extraction of the fixed cells. In unchallenged cells, XRCC1 was primarily found in the chromatin fraction in a highly phosphorylated form; in addition, a minor population (10 - 15%) existed in the nuclear matrix (NM) with no or marginal phosphorylation. After hydrogen peroxide treatment, hyperphosphorylated XRCC1 appeared in the NM and accordingly, those in the chromatin fraction decreased. Foci formation and changes in XRCC1 distribution could be abolished by the knockdown of CK2, the expression of a non-phosphorylatable version of XRCC1, or the inhibition of poly-ADP ribosylation at the damage sites. Other BER factors, like DNA polymerase β, were also found to accumulate in the NM after hydrogen peroxide-induced DNA damage, although its association with the NM seemed relatively weak. Our results suggest that the constitutive phosphorylation of XRCC1 in the chromatin and its DNA damage-induced recruitment to the NM are critical for foci formation, and that the core reactions of BER/SSBR may occur in the NM.

1. INTRODUCTION

In a mammalian cell, several thousands of spontaneous oxidation, alkylation and hydrolysis reactions occur in DNA molecules each day [1]. This extensive damage is rapidly repaired by a base excision repair/single strand break repair (BER/SSBR) system. Without the highly effective BER/SSBR system, accumulated damage or repair intermediates would interfere with replication or transcription machinery and devastate cell viability [2]. Several BER/SSBR proteins have been observed to assemble and form dense foci in the nucleus after DNA damage occurred [3, 4, 5], and these foci are considered to be critical for efficient DNA repair. The mechanisms that enable the assembly and release of BER/SSBR proteins at the nuclear foci are still unclear; however, specific protein-protein interactions may play a crucial role [6]. For example, XRCC1 specifically interacts with poly (ADP-ribose) polymerase-1 (PARP1) [7], which recognizes nicks in DNA. XRCC1 also interacts with other BER/SSBR factors, including 8-oxoguanine DNA glycosylase (OGG1) [8], DNA polymerase β (Pol β) [9, 10], DNA ligase IIIα (LIG3α) [11, 12], and polynucleotide kinase (PNK) [13]. Based on its multiple interactions and no known biochemical activities, XRCC1 has been proposed to function as a scaffold that brings together other factors and thereby facilitates BER/SSBR.

DNA metabolism, including DNA replication, transcription, recombination, and nucleotide excision repair (NER), appears to proceed through the actions of macro-molecular complexes that are localized in the non-chromatin compartment of the nucleus, or the nuclear matrix (NM). Rad51, BRCA1, and BRCA2, which function in DNA double strand break repair, are associated with the NM and their levels increase in response to DNA damage [14, 15]. Proteins involved in the NER reaction are recruited to the NM immediately after UV irradiation and form foci; this suggests that the repair reaction occurs in the NM [16, 17]. Some of the proteins involved in BER/SSBR, including OGG1 and PARP1, have been reported to associate with the NM [18, 19]. However, how accumulation of repair proteins in the NM is regulated and contributes to the efficient repair reaction is currently unclear.

To investigate the mechanism underlying foci formation in BER/SSBR, we analyzed the subnuclear localization of XRCC1. Here we showed that in response to H_2O_2 exposure, XRCC1 appeared to translocate from the chromatin to the NM and form foci. This NM translocation and foci formation required that XRCC1 was first phosphorylated in the chromatin. These data imply that a phosphorylation-based mechanism controls the localization of XRCC1 in response to DNA damage to function as a scaffold for BER/SSBR.

2. MATERIALS AND METHODS

2.1. Cell culture, plasmids, and transfection

HeLa cells were grown on plastic dishes in Dulbecco's modified Eagle's medium (Sigma) supplemented with 10% fetal bovine serum (FBS) in 5% CO_2 at 37˚C. CHO cells (AA8 and EM9) were cultured in α-MEM (Sigma) containing 10% FBS. The expression construct for wild-type XRCC1 (pCMVXRCC1^{WT}) was described in a previous study [20]. The CK2-site mutated XRCC1 cDNA derived from pcD2EXH^{CKM} [21] was cloned into the pCMV vector. Expression plasmids were introduced into XRCC1-deficient EM9 cells using Effectene (Qiagen) and selected with G418 (1.6 mg/ml). Two clones that expressed XRCC1 at the same level as the AA8 wild-type cells were isolated for each construct. The resulting EM9 cells that expressed wild-type and CK2-site mutant XRCC1 were designated as WT and CKM cells, respectively. For the knockdown studies, 48 hr transfections were performed with HiPerFect (Qiagen) mixed with negative control or CK2α specific (Qiagen) siRNA oligonucleotides at a concentration of 5 nM. The oligonucleotide sense strand sequences were as follows: negative control, UUCUCCGAACGUGUCACGUdTdT; Hs_CSNK2A1_9_HP validated, CUGGACUUCCAGAAGAACAdTdT; and Hs_CSNK2A1_11_HP, GAUCUAACCCUAAAUCCAAdTdT.

2.2. Fractionation of nuclear proteins and preparation of the nuclear matrix

Because different procedures have been reported for NM preparation, two fractionation methods were employed; a high-salt extraction [22] and a sequential extraction [17, 23].

High salt extraction. Cells were harvested by trypsinization and 2× to 3×10^6 cells were washed with PBS, suspended in 200 μl CSK buffer (10 mM PIPES, pH 6.8, 100 mM NaCl, 300 mM sucrose, 3 mM $MgCl_2$, 1 mM EGTA, 0.5% Triton X-100), and incubated on ice for 5 min. Soluble proteins were collected after centrifugation at 5,000×*g* for 3 min (Figs. 1A and B, high-salt, soluble). Pellets were suspended in 50 μl CSK buffer containing 50 units of RNase free-DNaseI (Takara) and Complete Protease Inhibitor Cocktail (Roche) and incubated at 37˚C for 15 min. Then, CSK buffer containing 1 M ammonium sulfate was added to the DNase reaction in order to obtain a final concentration of 0.25 M ammonium sulfate, and the reaction was incubated on ice for 5 min. Chromatin fractions were collected after centrifugation at 5,000×*g* for 3 min (Figs. 1A and B, high-salt, chromatin). The pellets were suspended in CSK buffer containing 2 M NaCl and incubated on ice for 5 min; the 2 M wash fraction was collected after centrifugation at 5,000×*g* for 3 min (Figs. 1A and B, high-salt, wash). The remaining nuclear matrix was solubilized in 20 μl of Reagent 3 solution (ReadyPrep™ Sequential Extraction kit; Bio Rad) containing 5 M urea and 2 M thiourea (Figs. 1A and B, high-salt, NM).

Sequential extraction method. Cells grown to semiconfluence were harvested by trypsinization and 8×10^5 cells were collected in a micro tube. The nuclear pellet was prepared as previously described [24]. The fractionation of nuclear proteins from the pellet was performed as described [17, 23] with slight modifications. Briefly, the nuclear pellet was washed with low salt buffer (10 mM Tris-HCl, pH 7.4, 0.2 mM $MgCl_2$, 1 mM PMSF) and preincubated in DNase digestion buffer (25 mM Tris-HCl, pH 7.4, 250 mM glucose, 5 mM $MgCl_2$, protease inhibitor cocktail set III [Calbiochem] without DNase) at 25˚C for 30 min and centrifuged at 14,000×*g* for 3 min. The pellet was resuspended in 50 μl DNase digestion buffer with 1 unit/μl RNase free-DNaseI (Takara) and incubated at 25˚C for 1 hr. The samples were centrifuged at 14,000×*g* for 3 min and the supernatant was collected (Figs. 1A and B, sequential, soluble). The precipitate was washed with the low salt buffer, extracted sequentially with the low-salt buffer containing increasing concentrations of NaCl (0.3, 0.5, and 2.0 M) for 15 min, and centrifuged at 15,000×*g* for 15 min (Figs. 1A and B; sequential; 0.3 M, 0.5M , and 2 M fractions, respectively). The final pellet was washed with the low-salt buffer and solubilized in 25 μl Reagent 3 solution (Figs. 1A and B, sequential, NM).

2.3. H_2O_2 treatment

To investigate changes in the protein localization among the fractions after DNA damage, cells were exposed to 150 μM or 10 mM H_2O_2 [21] added in fresh medium without FBS for 10 min at 37˚C. The cells were washed twice with PBS and incubated in medium with FBS for 10 min before collection. For the immunofluorescent staining of poly (ADP-ribose) (PAR), cells were incubated for 2 min before fixation. To inhibit PARP1, 3-aminobenzamide (3AB) was added to the culture medium at a final concentration of 8 mM and incubated for 90 min before H_2O_2 exposure. 3AB was also added to the media for the H_2O_2 exposure and for the post-exposure incubation.

2.4. Western blotting analysis

Aliquots of 5×10^5 cells were boiled in SDS sample buffer for all but one fraction; aliquots of the fraction solubilized with Reagent 3 were mixed with SDS sample buffer without boiling. The samples were applied to 10% or 5-20% gradient polyacrylamide gels. To verify that CK2α was knocked down, 3×10^5 cells were harvested and cytoplasmic proteins were extracted with a Nuclear Extract kit (Active Motif). The nuclear pellet was washed with PBS, suspended with PBS containing DNaseI (0.1 units/μl), and incubated for 30 min at 30˚C. The nuclear suspension was mixed with SDS sample buffer and boiled. The primary antibodies and dilutions used in the experiments were: Anti-XRCC1 (1:500; Lab Vision), anti-LIG3α (1:1000; GeneTex), anti-proliferating cell nuclear antigen (PCNA) (1:1000; Lab Vision), anti-Lamin B (1:500; Progen) anti-PARP1 (1:2000; R&D Systems), anti-OGG1 (1:100; IBL, Japan), anti-Pol β (1:200; Lab Vision), anti-APE1 (1:500; R&D Systems), and anti-CK2α (1:1000; New England Biolabs, Inc.). Horseradish peroxidase (HRP)-labeled secondary antibodies were purchased from GE Healthcare. Proteins were detected by ECL plus and ECL film (GE Healthcare); the band intensities were quantified by ImageJ software (http://rsb.info.nih.gov/ij/) and normalized with respect to Lamin B (for the NM fraction) or histones detected by CBB staining of the filter used for the Western blotting (for the chromatin fraction).

2.5. In situ extraction and immunofluorescent staining

To analyze the location of NM protein in the cells, we performed *in situ* extraction on cells attached to glass slides. The *in situ* extraction procedure was basically the same as the sequential extraction method used for protein fractionation. HeLa cells (8×10^3) were seeded into each well of an 8-well chamber slide (Nunc) and incubated for 2 days. The cells were washed with PBS and fixed with ice-cold methanol/acetone (1:1) on ice for 10 min. After the glass slides were dried, the cells were rehydrated by incubating in PBS on ice for 10 min. To remove cytoplasmic proteins, the cells were incubated for 5 min on ice in hypotonic buffer containing 0.05% Triton X-100. Chromosomal DNA was digested with 1 unit/μl DNaseI in DNase digestion buffer at 30˚C for 1 hr. Nuclear proteins were extracted sequentially with the low-salt buffer containing increasing concentrations of NaCl (0.3, 0.5, and 2.0 M) and protease inhibitor for 10 min on ice. After blocking with 2% BSA in PBS for 1 hr, the cells were incubated with anti-XRCC1 antibody (1:200; Bethyl laboratories Inc.) and/or anti-PAR antibody (1:200; Trevigen) in 2% BSA/PBS for 20 min at 37˚C. After washing twice with PBS, cells were incubated with TRITC-conjugated anti-mouse IgG (Sigma) and/or FITC-conjugated anti-rabbit IgG (Sigma) in 2% BSA in PBS overnight at 4˚C. The slides were washed five times with PBS and sealed with ProLong Gold antifade reagent containing DAPI (Molecular Probes), and cover slips were placed over the slides. To check the extraction of DNA and nuclear proteins, DAPI and anti-PCNA antibody (1:500; Santa Cruz) staining was performed. For *in vivo* cross-linking, H_2O_2-treated cells were washed with PBS and incubated in 1.25 mM Dithiobis (succinimidylpropionate) (DSP; PIERCE, 50 mM in dimethylsulfoxide) in PBS at room temperature for 10 min, and then cells were subjected to *in situ* extraction. Cell images were captured and analyzed with a Zeiss LSM 510 Confocal Microscope, Axioplan2, and Zeiss LSM imaging software. The images were taken at 20× or 63× magnification.

2.6. Phosphatase treatment and 2D electrophoresis

To analyze the phosphorylation status of the XRCC1 protein, the buffer of the chromatin fraction from 2×10^6 cells was exchanged with λ-protein phosphatase (λ-PPase) reaction buffer (50 mM HEPES, pH 7.5, 0.1 mM EDTA, 5 mM DTT, 0.01% Brij 35) with a microcon tube (Millipore). Then, $MnCl_2$ and λ-PPase (New England Biolabs Inc.) were added at concentrations of 2 mM and 200 units/μl, respectively, and the reaction mixture was incubated for 1 hr at 30˚C. An additional aliquot of λ-PPase (400 units/μl final) was added to the reaction and incubated for an additional 1 hr. As a negative control for dephosphorylation, samples without λ-PPase were combined with phosphatase inhibitor cocktail set II (Calbiochem) and incubated in the same manner. The NM pellet was suspended in λ-PPase reaction buffer and incubated with or without λ-PPase as described above. The proteins were desalted and the buffers replaced with 2D electrophoresis buffer (7 M urea, 2 M thiourea and 4% CHAPS) with protein desalting spin columns (Pierce). The samples were mixed with DTT, IPG buffer (pH 3-10NL, GE Healthcare), and bromophenol blue and applied to an Immobiline gel pH 3-10NL (GE Healthcare). Isoelectric focusing (IEF) was performed with a programmed protocol of 50V for 12 hrs for rehydration, and then 200 V for 30 min, 600 V for 30 min, and 2,000 V for 8 hrs for focusing.

Second-dimension separation was performed by SDS-PAGE with 8% polyacrylamide gels. The detection of XRCC1 protein by Western blotting was carried out as described in section 2.4.

3. RESULTS

3.1. Subcellular localization of XRCC1 proteins

HeLa cellular proteins were fractionated by either high-salt or sequential extraction methods (Fig. 1A). A typical Western blot of the fractions is shown in Figure 1B. PCNA was detected primarily in the soluble and chromatin fractions and was faintly evident in the NM; Lamin B resided exclusively in the NM, in agreement with previous observations [25,26], which confirmed the quality of the fractionation. Histones were observed mainly in the chromatin fraction that was isolated with the high-salt method and in the 0.5 M and 2 M NaCl fractions isolated with the sequential method. Large proportions of XRCC1 were found in the chromatin fraction obtained with the high-salt method (approximately 75%) or in the fractions extracted with 0.5 M and 2 M NaCl of the sequential extraction method (approximately 60%). Soluble XRCC1, typically extracted with 100 - 300 mM NaCl and used in immunoprecipitation experiments, comprised a lesser component; approximately 15% of the total XRCC1 was soluble with the high-salt method and approximately 25% (0.3 M fraction) was soluble with the sequential method. Interestingly, roughly 11% and 15% of XRCC1 was found in the NM with the high-salt and sequential methods, respectively. A substantial amount of LIG3α was also observed in the NM.

We also probed for other BER/SSBR proteins in each fraction obtained with the high-salt method. Nuclear type OGG1 was detected in the soluble, chromatin, and NM fractions as previously reported [18]. Similar distribution patterns were found for Pol β and AP endonuclease 1 (APE1) proteins, except they exhibited a very faint or no signal in the NM. PARP1 was detected largely in the soluble (45%) and chromatin (35%) fractions, but approximately 12% and 8% also existed in the wash and NM fractions, respectively.

3.2. XRCC1 protein in the nuclear matrix fraction increases following oxidative damage

To examine whether induction of oxidative DNA damage affected the subnuclear localization of XRCC1, HeLa cells were exposed to 150 μM H_2O_2, which resulted in 20% colony forming ability. Then we analyzed the amounts of XRCC1 in the NM and chromatin fractions (Figs. 1C and D). Both extraction methods gave essentially the same results; however, the change in protein distribution in response to H_2O_2 was more evident with the high-salt method. After exposure to H_2O_2, the XRCC1 level increased by 2.5-fold in the NM with a concomitant reduction in the chromatin fraction. LIG3α showed a similar change in distribution. This redistribution appeared to be a transient phenomenon because the XRCC1 levels in the NM returned to basal values within 3 hours (data not shown). This coincides with foci formation kinetics previously reported [27].

3.3. Phosphorylation by CK2 is responsible for the increase of XRCC1 in the nuclear matrix

Next we examined the possibility that CK2 may regulate the accumulation of XRCC1 in the NM; phosphorylation by CK2 has been shown to be critical for foci formation after H_2O_2 [21]. To test this hypothesis, siRNA was specifically directed against the catalytic α subunit of CK2 and the amount of XRCC1 was analyzed in the NM fractionated with the high-salt method. Transfection with either of the two different siRNAs for CK2α reduced cellular CK2α protein levels to roughly 25% of control in both the cytosol and nucleus (Fig. 2A). This reduction in CK2α did not affect the total amount of XRCC1 in the nucleus or the overall protein profile, although the basal amount of XRCC1 in the NM was slightly reduced by knocking down CK2α (Fig. 2B and C, H_2O_2 -). Interestingly, the increase of XRCC1 in the NM after H_2O_2 exposure was completely inhibited by the CK2α knockdown (Fig. 2B and C, H_2O_2 +). To confirm these results, we examined the effect of expressing in the EM9 cells a mutant XRCC1 (XRCC1^{CKM}), where all eight phosphorylation sites were changed to alanine [21]. The mutation did not cause an apparent change in the XRCC1 distribution in the absence of H_2O_2 treatment (data not shown) or in the basal level of XRCC1 in the NM (Fig. 2D and E, H_2O_2 -). Notably, when cells were exposed to H_2O_2, the level of XRCC1^{WT} increased in the NM, but the level of XRCC1^{CKM} remained unchanged (Fig. 2D and E, H_2O_2 +), in good agreement with the knockdown experiment. These results suggested that phosphorylation by CK2 was required for the increase of XRCC1 in the NM after H_2O_2 exposure (see Discussion). Because this experiment used XRCC1 with a non-native promoter, the results support the notion that post-translational regulation, but not the induction of gene expression, was responsible for the increase of XRCC1 in the NM.

3.4. Highly phosphorylated form of XRCC1 in the nuclear matrix appeared after H_2O_2 treatment in a CK2-dependent manner

We next analyzed the phosphorylation status of $XRCC1^{WT}$ and $XRCC1^{CKM}$ proteins in each fraction in response to H_2O_2 treatment. The WT and CKM cells were incubated in the presence or absence of H_2O_2, followed by the fractionation of the cellular proteins by the high-salt method, separated by 2D gel electrophoresis and probed for XRCC1. The XRCC1 in the chromatin and NM fractions were detected as spots at different pI positions indicating different phosphorylation statuses (Fig. 3). Lanes 9 and 10 show the position of completely unphosphorylated XRCC1. Interestingly, the XRCC1 in the chromatin fraction was highly phosphorylated without H_2O_2 treatment (lane 1), but the XRCC1 in the NM did not appear to be phosphorylated (lane 5). A spot-shift was barely detectable in the CKM cells (lane 3) suggesting that the phosphorylation almost exclusively depended on CK2. After H_2O_2 treatment, the XRCC1 in the chromatin appeared at a slightly reduced pI position (lanes 2), but the significance of this is not clear. The most striking change was the appearance of a hyperphosphorylated XRCC1 in the NM fraction (lane 6). Together with the observation that XRCC1 increased in the NM and concomitantly decreased in the chromatin after H_2O_2 treatment (Figs. 1C and 2E), these results suggest that phosphorylated XRCC1 was recruited to the NM from the chromatin and CK2-dependent phosphorylation was a prerequisite for the relocation (see Discussion). We also observed intermediately phosphorylated XRCC1 in the NM after H_2O_2 treatment (lane 6), however its origin is currently unknown (see Discussion).

3.5. XRCC1 foci resistant to in situ extraction are increased by H_2O_2 treatment

XRCC1 has been shown to form nuclear foci after treatment with alkylating agents or H_2O_2 [24, 27], and foci formation is considered indicative of ongoing BER/SSBR [3]. The damage dependent accumulation of XRCC1-LIG3α observed in the NM (Fig 1C and D) suggested the possibility that the BER/SSBR reaction may be conducted in the NM. This notion was corroborated by determining whether XRCC1 foci were associated with the NM. Cells grown on glass slides were sequentially treated with Triton X-100, DNaseI, and 0.3, 0.5, and 2 M NaCl, essentially the sequential extraction method applied in the fractionation study (Fig. 1B). Both DAPI and PCNA staining confirmed the absence of DNA and soluble/chromatin proteins in the *in situ* extracted cells (Fig. 4A). A diffuse distribution of the XRCC1 protein was observed in the nucleus of unchallenged cells even after *in situ* extraction (Fig. 4B, green signal), suggesting a damage-independent association of XRCC1 with the NM. Notably, XRCC1 foci that formed after H_2O_2 treatment were also resistant to *in situ* extraction (Fig. 4B, XRCC1^{WT}, H_2O_2 +). Although foci-like structures were also observed in untreated cells, the H_2O_2 treatment increased the number of foci and made them more distinct. This finding is consistent with the data from the biochemical fractionation analyses (Fig. 1D).

To examine whether XRCC1 foci were formed at the damaged site, we immunostained HeLa cells with antibodies specific for PAR, which is synthesized by PARP at DNA nicks [27, 28]. Extraction-resistant PAR foci were detected in a manner absolutely dependent on H_2O_2 treatment (Fig. 4B red signal); moreover the XRCC1^{WT} and PAR foci were co-localized (Fig. 4B, XRCC1^{WT}, H_2O_2 +). In contrast, in CKM cells, XRCC1^{CKM} protein did not form distinct foci after H_2O_2 exposure (Fig. 4B, XRCC1^{CKM}, H_2O_2 +), consistent with the previous report [21]. When cells were pretreated with the PARP inhibitor, 3AB, H_2O_2 treatment did not lead to an increase of XRCC1 in the NM (Fig. 5A); thus, PARP1 activity was critical for the accumulation. Moreover, in the *in situ* extracted cells, 3AB inhibited formation of both the PAR and XRCC1 foci (Fig. 5B). Interestingly, PAR localization was also affected in CKM cells, where PAR showed diffuse distribution pattern (Fig. 4B, XRCC1^{CKM}, H_2O_2 +). These results suggest that PAR foci formation in the NM is also regulated through phosphorylation of XRCC1, at least to some extent (see Discussion).

We found Pol β in the soluble and chromatin fractions, but not in the NM (Fig. 1B). This was inconsistent with our hypothesis that BER/SSBR may take place in the NM. We then hypothesized that this may have been due to a weak association between Pol β and XRCC1/damaged DNA/NM. To investigate this possibility, cells were exposed to H_2O_2, treated with the *in vivo* cross-linking reagent, DSP, extracted *in situ*, and XRCC1 and Pol β were examined. Hydrogen peroxide clearly induced a distinct localization of Pol β that is resistant to *in situ* extraction, and more than half of the Pol β had co-localized with XRCC1 (Fig. 6). Some Pol β that did not show co-localization may represent XRCC1-independent accumulation at oxidative DNA damage [3]. Although it is formally possible that cross-linking may have picked up false interactions, the damage dependence and co-localization with XRCC1 suggest an actual association of Pol β with the NM. Taken together, these results suggest that BER/SSBR may occur in the NM.

4. DISCUSSION

The NM consists of a nuclear lamina and a network of nuclear proteins. It is proposed to provide a platform for certain aspects of DNA metabolism [29], including repair of UV damaged [17] or cross-linked DNA [30], and recombination [14]. BER/SSBR has not previously been intensely studied in terms of its relation to the NM. In the present study, we showed that XRCC1 protein accumulated in the NM in a damage-dependent manner, and that several treatments known to abolish repair activity or foci formation of XRCC1 also compromised its accumulation in the NM. In addition, XRCC1 foci that co-localized with PAR were resistant to the *in situ* extraction procedure that removed the soluble and chromatin fraction of cellular proteins. Although direct proof is lacking, out data suggest that XRCC1 functions in the NM during the BER/SSBR reaction. Whether BER/SSBR really occurs in the NM is a difficult question to address. Some proteins that reside in the NM fraction have shown activity in a reconstituted BER reaction [31, 32], but it is not clear whether this truly reflects their function in repair activity in the NM. For a more compelling argument, an *in situ* repair assay for the NM should be devised.

The XRCC1 proteins existed both in the chromatin and in the NM, and exhibited different phosphorylation statuses in unchallenged cells (Fig. 3). Although virtually all XRCC1 in the chromatin was hyperphosphorylated, phosphorylation was not required for the localization to the chromatin. Notably, H_2O_2 treatment led to a reduction of hyperphosphorylated XRCC1 in the chromatin and a concomitant appearance in the NM. This observation is best explained by assuming a damage-triggered recruitment of XRCC1 from the chromatin to the NM. Our preliminary observation suggested that CK2 did not reside in the NM under the present conditions (Kubota, unpublished result), consistent with the chromatin origin of hyperphosphorylated XRCC1 (but see also [33, 34]). The recruitment of XRCC1 to the NM appeared to be absolutely dependent on phosphorylation by CK2 prior to H_2O_2 treatment. Thus, in this scenario, chromatin functions as a reservoir for hyperphosphorylated XRCC1. Intriguingly, non-phosphorylated XRCC1 that resides in the NM irrespective of H_2O_2 treatment did not seem to be involved in foci formation. This is consistent with its inability to interact with other repair factors [21]. After H_2O_2 treatment, we also observed several spots of intermediately phosphorylated XRCC1. The source of these spots is currently unknown. One possibility is that XRCC1 is dephosphorylated after the repair reaction by a presumably NM-associated phosphatase activity. This remains to be explored in a future study.

It has been well established that the localization of XRCC1 to damaged DNA is dependent on PARP activity, and XRCC1 foci are formed via interaction with PAR (Fig. 5B, [27]). However, in our experiment, the pattern of extraction-resistant PAR foci was also affected by the phosphorylation of XRCC1 by CK2 (Fig. 4B). Consistent with this, the XRCC1 knockdown impaired PAR foci formation in the NM (Kubota, unpublished observation). These observations suggest the following scenario. XRCC1 in the chromatin is constitutively phosphorylated by CK2 in preparation for future DNA damage. When cells are exposed to H_2O_2, PAR is formed in the vicinity of the damage. Subsequently, XRCC1 accumulates at the damage site through an interaction with PAR, and the ternary complex is transported to the NM for the repair reaction. This accounts for the defect in formation of extraction-resistant PAR foci in CKM cells. Other repair factors might be localized to the damage sites after the XRCC1 scaffold has been established in the NM. Thus, the impaired distribution of PAR and XRCC1^{CKM} shown in Figure 4B may contribute to the slower repair of single strand breaks in CKM cells [21]. Further investigation is needed to clarify the correlation between the molecular mechanism of XRCC1 foci-formation and BER/SSBR activity of cells.

Although CK2 was classically considered to be a ubiquitous kinase with no specific regulatory role, an increasing number of reports have provided evidence that CK2 is a key player in various stress responses [35]. For example, histone H4 serine 1 is reported to be phosphorylated by CK2 in response to double strand breaks in yeast [36]. On the other hand, BER/SSBR has been long regarded as a simple, constitutive reaction that did not require regulation. However, recent work has proposed several regulation mechanisms involving XRCC1 for the BER/SSBR response to DNA damage [37, 38]. Interestingly, the assembly of OGG1 into nuclear speckles is not initiated by DNA damage but, rather, by reactive oxygen species and signal transduction [39]. Furthermore, OGG1 is activated by phosphorylation by PKC, cdk4 and c-Abl [18, 40]. These reports suggest a possibility that the initiation of BER/SSBR is under active regulation, probably by a phosphorylation cascade. Our findings provide an example of BER/SSBR regulation by CK2, where phosphorylation plays a preemptive role in preparation for damage induction by ensuring an adequate supply of functional repair proteins for a rapid repair response.

Conflict of Interest statement

None.

Acknowledgments

The plasmid pcD2EXH^{CKM} was a gift from Dr. Keith Caldecott. The Ministry of Education, Culture, Sports, Science and Technology, Japan, 'Open Research Center' Project for Private Universities, 2004-2008 funded the work carried out by Y.K. and T.T.

REFERENCES

[1] E. C. Friedberg, G. C. Walker, W. Siede, R. D. Wood, R. A. Schultz, T. Ellenberger. DNA Repair and Mutagenesis, ASM Press, Washington, DC, 2005.

[2] J. C. Harrison, J. E. Haber. Surviving the breakup: the DNA damage checkpoint, Annu Rev Genet 40 (2006) 209-235.

[3] L. Lan, S. Nakajima, Y. Oohata, M. Takao, S. Okano, M. Masutani, S. H. Wilson, A. Yasui. In situ analysis of repair processes for oxidative DNA damage in mammalian cells, Proc Natl Acad Sci USA 101 (2004) 13738-13743.

[4] R. M. Taylor, D. J. Moore, J. Whitehouse, P. Johnson, K. W. Caldecott. A cell cycle-specific requirement for the XRCC1 BRCT II domain during mammalian DNA strand break repair, Mol Cell Biol 20 (2000) 735-740.

[5] J. Fan, M. Otterlei, H. K. Wong, A. E. Tomkinson, D. M. Wilson. XRCC1 co-localizes and physically interacts with PCNA, Nucleic Acids Res 32 (2004) 2193-2201.

[6] K. H. Almeida, R. W. Sobol. A unified view of base excision repair: lesion-dependent protein complexes regulated by post-translational modification, DNA Repair (Amst) 6 (2007) 695-711.

[7] M. Masson, C. Niedergang, V. Schreiber, S. Muller, J. Menissier-de Murcia, G. de Murcia. XRCC1 is specifically associated with poly(ADP-ribose) polymerase and negatively regulates its activity following DNA damage, Mol Cell Biol 18 (1998) 3563-3571.

[8] S. Marsin, A. E. Vidal, M. Sossou, J. Ménissier-de Murcia, F. Le Page, S. Boiteux, G. de Murcia, J. P. Radicella. Role of XRCC1 in the coordination and stimulation of oxidative DNA damage repair initiated by the DNA glycosylase hOGG1, J Biol Chem 278 (2003) 44068-44074.

[9] Y. Kubota, R. A. Nash, A. Klungland, P. Schär, D. E. Barnes, T. Lindahl. Reconstitution of DNA base excision-repair with purified human proteins: interaction between DNA polymerase beta and the XRCC1 protein, EMBO J 15 (1996) 6662-6670.

[10] K. W. Caldecott, S. Aoufouchi, P. Johnson, S. Shall. XRCC1 polypeptide interacts with DNA polymerase beta and possibly poly (ADP-ribose) polymerase, and DNA ligase III is a novel molecular 'nick-sensor' in vitro, Nucleic Acids Res 24 (1996) 4387-4394.

[11] K. W. Caldecott, C. K. McKeown, J. D. Tucker, S. Ljungquist, L. H. Thompson. An interaction between the mammalian DNA repair protein XRCC1 and DNA ligase III, Mol Cell Biol 14 (1994) 68-76.

[12] K. W. Caldecott, J. D. Tucker, L. H. Stanker, L. H. Thompson. Characterization of the XRCC1-DNA ligase III complex in vitro and its absence from mutant hamster cells, Nucleic Acids Res 23 (1995) 4836-4843.

[13] C. J. Whitehouse, R. M. Taylor, A. Thistlethwaite, H. Zhang, F. Karimi-Busheri, D. D. Lasko, M. Weinfeld, K. W. Caldecott. XRCC1 stimulates human polynucleotide kinase activity at

damaged DNA termini and accelerates DNA single-strand break repair, Cell 104 (2001) 107-117.

[14] E. Mladenov, B. Anachkova, I. Tsaneva. Sub-nuclear localization of Rad51 in response to DNA damage, Genes Cells 11 (2006) 513-524.

[15] L. J. Huber, L. A. Chodosh. Dynamics of DNA repair suggested by the subcellular localization of Brca1 and Brca2 proteins, J Cell Biochem 96 (2005) 47-55.

[16] D. R. Koehler, P. C. Hanawalt. Recruitment of damaged DNA to the nuclear matrix in hamster cells following ultraviolet irradiation, Nucleic Acids Res 24 (1996) 2877-2884.

[17] S. Kamiuchi, M. Saijo, E. Citterio, M. de Jager, J. H. Hoeijmakers, K. Tanaka. Translocation of Cockayne syndrome group A protein to the nuclear matrix: possible relevance to transcription-coupled DNA repair, Proc Natl Acad Sci U S A 99 (2002) 201-206.

[18] F. Dantzer, L. Luna, M. Bjoras, E. Seeberg. Human OGG1 undergoes serine phosphorylation and associates with the nuclear matrix and mitotic chromatin in vivo, Nucleic Acids Res 30 (2002) 2349-2357.

[19] M. R. Mennella, G. Roma, B. Farina. Active poly(ADPribose) metabolism in DNase- and salt-resistant rat testis chromatin with high transcriptional activity/competence, J Cell Biochem 89 (2003) 688-697.

[20] Y. Kubota, S. Horiuchi. Independent roles of XRCC1's two BRCT motifs in recovery from methylation damage, DNA Repair (Amst) 2 (2003) 407-415.

[21] J. I. Loizou, S. F. El-Khamisy, A. Zlatanou, D. J. Moore, D. W. Chan, J. Qin, S. Sarno, F. Meggio, L. A. Pinna, K. W. Caldecott. The protein kinase CK2 facilitates repair of chromosomal DNA single-strand breaks, Cell 117 (2004) 17-28.

[22] D. C. He, J. A. Nickerson, S. Penman. Core filaments of the nuclear matrix, J Cell Biol 110 (1990) 569-580.

[23] V. R. Otrin, M. McLenigan, M. Takao, A. S. Levine, M. Protic. Translocation of a UV-damaged DNA binding protein into a tight association with chromatin after treatment of mammalian cells with UV light, J Cell Sci 110 (1997) 1159-1168.

[24] T. Takanami, J. Nakamura, Y. Kubota, S. Horiuchi. The Arg280His polymorphism in X-ray repair cross-complementing gene 1 impairs DNA repair ability, Mutat Res 582 (2005) 135-145.

[25] P. Hozak, D. A. Jackson, P. R. Cook. Replication factories and nuclear bodies: the ultrastructural characterization of replication sites during the cell cycle, J Cell Sci 107 (1994) 2191-2202.

[26] Y. Gruenbaum, K. L. Wilson, A. Harel, M. Goldberg, M. Cohen. Review: nuclear lamins--structural proteins with fundamental functions, J Struct Biol 129 (2000) 313-323.

[27] S. F. El-Khamisy, M. Masutani, H. Suzuki, K. W. Caldecott. A requirement for PARP-1 for the assembly or stability of XRCC1 nuclear foci at sites of oxidative DNA damage, Nucleic Acids Res 31 (2003) 5526-5533.

[28] T. Lindahl, M. S. Satoh, G. G. Poirier, A. Klungland. Post-translational modification of poly(ADP-ribose) polymerase induced by DNA strand breaks, Trends Biochem Sci 20 (1995) 405-411.

[29] G. S. Stein, S. K. Zaidi, C. D. Braastad, M. Montecino, A. J. van Wijnen, J. Y. Choi, J. L. Stein, J. B. Lian, A. Javed. Functional architecture of the nucleus: organizing the regulatory machinery for gene expression, replication and repair, Trends Cell Biol 13 (2003) 584-592.

[30] F. Qiao, A. Moss, G. M. Kupfer. Fanconi anemia proteins localize to chromatin and the nuclear matrix in a DNA damage- and cell cycle-regulated manner, J Biol Chem 276 (2001) 23391-23396.

[31] D. M. r. Wilson, W. A. Deutsch, M. R. Kelley. Drosophila ribosomal protein S3 contains an activity that cleaves DNA at apurinic/apyrimidinic sites, J Biol Chem 269 (1994) 25359-25364.

[32] A. Yacoub, L. Augeri, M. R. Kelley, P. W. Doetsch, W. A. Deutsch. A Drosophila ribosomal protein contains 8-oxoguanine and abasic site DNA repair activities, EMBO J 15 (1996) 2306-2312.

[33] H. Wang, S. Yu, A. T. Davis, K. Ahmed. Cell cycle dependent regulation of protein kinase CK2 signaling to the nuclear matrix, J Cell Biochem 88 (2003)

[34] P. Hilgard, T. Huang, A. W. Wolkoff, R. J. Stockert. Translated Alu sequence determines nuclear localization of a novel catalytic subunit of casein kinase 2, Am J Physiol, Cell Physiol 283 (2002) 472-483.

[35] K. Ahmed. Joining the cell survival squad: an emerging role for protein kinase CK2, Trends Cell Biol 12 (2002) 226-230.

[36] W. L. Cheung, F. B. Turner, T. Krishnamoorthy, B. Wolner, S. H. Ahn, M. Foley, J. A. Dorsey, C. L. Peterson, S. L. Berger, C. D. Allis. Phosphorylation of histone H4 serine 1 during DNA damage requires casein kinase II in S. cerevisiae, Curr Biol 15 (2005) 656-660.

[37] J. L. Parsons, P. S. Tait, D. Finch, I. I. Dianova, S. L. Allinson, G. L. Dianov. CHIP-Mediated Degradation and DNA Damage-Dependent Stabilization Regulate Base Excision Repair Proteins, Mol Cell 29 (2008) 477-487.

[38] W. Chou, H. Wang, F. Wong, S. Ding, P. Wu, S. Shieh, C. Shen. Chk2-dependent phosphorylation of XRCC1 in the DNA damage response promotes base excision repair, The EMBO Journal 27 (2008) 3140-3150.

[39] A. Campalans, R. Amouroux, A. Bravard, B. Epe, J. P. Radicella. UVA irradiation induces relocalisation of the DNA repair protein hOGG1 to nuclear speckles, J Cell Sci 120 (2007) 23-32.

[40] J. Hu, S. Z. Imam, K. Hashiguchi, N. C. de Souza-Pinto, V. A. Bohr. Phosphorylation of human oxoguanine DNA glycosylase (alpha-OGG1) modulates its function, Nucleic Acids Res 33 (2005) 3271-3282.

FIGURE LEGENDS

Fig. 1. Detection of XRCC1 and LIG3α in the NM fraction. (**A**) HeLa cell proteins were fractionated by either high-salt or sequential extraction methods as described in the Materials and Methods. (**B**) Proteins fractionated by each method were applied to SDS-PAGE. XRCC1, LIG3α, PCNA and Lamin B were detected by Western blotting. Histones were detected by CBB staining of the SDS-PAGE gel. The distributions of the BER/SSBR proteins, PARP1, OGG1, Pol β, and APE1

obtained with the high-salt method are also shown. Arrowheads indicate histones. (**C**) XRCC1 and LIG3α were increased in the NM and reduced in the chromatin after H_2O_2 treatment. HeLa cells were exposed to 0 or 150 μM H_2O_2 for 10 min (- and +, respectively). After recovery, the NM and chromatin proteins were prepared with the high-salt method. XRCC, LIG3α and Lamin B were detected by Western blotting. (**D**) Quantification of the band intensity of XRCC1 in panel C. Band intensity was normalized to that of Lamin B, and the amount from cells in a control not treated with H_2O_2 was plotted as 1.0. The mean ± standard deviation of three experiments is shown (*p<0.05).

Fig. 2. Involvement of CK2 in the increase of XRCC1 in the NM. (**A**) Transfection with CK2α siRNA reduced cellular CK2α protein levels, but not XRCC1 levels. HeLa cells were transfected with the negative control (NegCnt) or siRNA for CK2α (CK2-1 and CK2-2, Hs_CSNK2A1_9_HP validated and Hs_CSNK2A1_11_HP, respectively), and incubated for 48 hours. Cytosolic (cyto.) and nuclear (nuc.) proteins corresponding to 3×10^4 cells were examined for CK2α and XRCC1 levels by Western blotting. CBB staining of the same Hybond-P filter used for the Western blotting is shown. (**B**) XRCC1 in the NM did not increase in CK2α knockdown cells (CK2) after H_2O_2 exposure. The cells were treated in the same way as in Fig. 1C and XRCC1 in the NM was analyzed by Western blotting. (**C**) Quantification of the band intensities in panel B. Band intensity was normalized to Lamin B and the amount from cells in a control not treated with H_2O_2 was plotted as 1.0. The mean ± standard deviation of two experiments is shown. (**D**) CK2 phosphorylation sites were responsible for the increase in XRCC1 in the NM after H_2O_2 exposure. EM9 cells expressing wild-type ($XRCC1^{WT}$) or the CK2 site mutant of XRCC1 ($XRCC1^{CKM}$) were exposed to 150 μM H_2O_2 and analyzed in the same way as in panel B. The results for EM9 cells harboring the empty vector (vec) are also shown. (**E**) Quantification of the band intensities of panel D. Band intensity was normalized to Lamin B and the amount from cells in a control not treated with H_2O_2 was plotted as 1.0. The mean ± standard deviation of two experiments is shown.

Fig. 3. Phosphorylation status of XRCC1 in each cellular fraction. WT or CKM cells were exposed to H_2O_2 as described in Fig. 1C, and proteins from each fraction were analyzed by 2D gel electrophoresis, followed by Western blotting. The position of non-phosphorylated XRCC1 is indicated by a portion of proteins from WT cells that was treated with λ-PPase, fractionated, and analyzed simultaneously (lanes 9 and 10).

Fig. 4. Co-localization of XRCC1 foci and PAR foci in the NM after H_2O_2 exposure. (**A**) *In situ* extraction removed chromosomal DNA (blue) and soluble/chromatin proteins (PCNA; red) from cells (extraction +/-). (**B**) WT and CKM cells were exposed to 0 or 10 mM H_2O_2 for 10 min, followed by 2 min of recovery. The cells were extracted *in situ*. DNA was detected by DAPI (blue). XRCC1 (green) and PAR (red) were immunostained with specific antibodies. The scale bar indicates 10 μm.

Fig. 5. PARP-dependent increase of XRCC1 in the NM after H_2O_2 exposure. (**A**) HeLa cells were treated with DMSO or 8 mM 3AB and exposed to H_2O_2 as described in Fig. 1C. XRCC1 in the NM was analyzed as described in Fig. 2B. (**B**) WT cells grown on LabTec chamber slides were treated with DMSO or 8 mM 3AB and exposed to 10 mM H_2O_2 for 10 min, followed by a 2-min repair period. Cells were extracted *in situ* as described in Fig. 4 and PAR (red) and XRCC1 (green) were immunostained with specific antibodies.

Fig. 6. Pol β foci formation in the NM after H_2O_2 exposure and co-localization with XRCC1 foci. WT cells were exposed to H_2O_2 as described in Fig. 1C, and cellular proteins were cross-linked *in vivo* by addition of DSP. The cells were washed and chromosomal DNA and soluble/chromatin proteins extracted *in situ*. Pol β (red) and XRCC1 (green) were detected in the NM by immunostaining with specific antibodies.

Figure 1

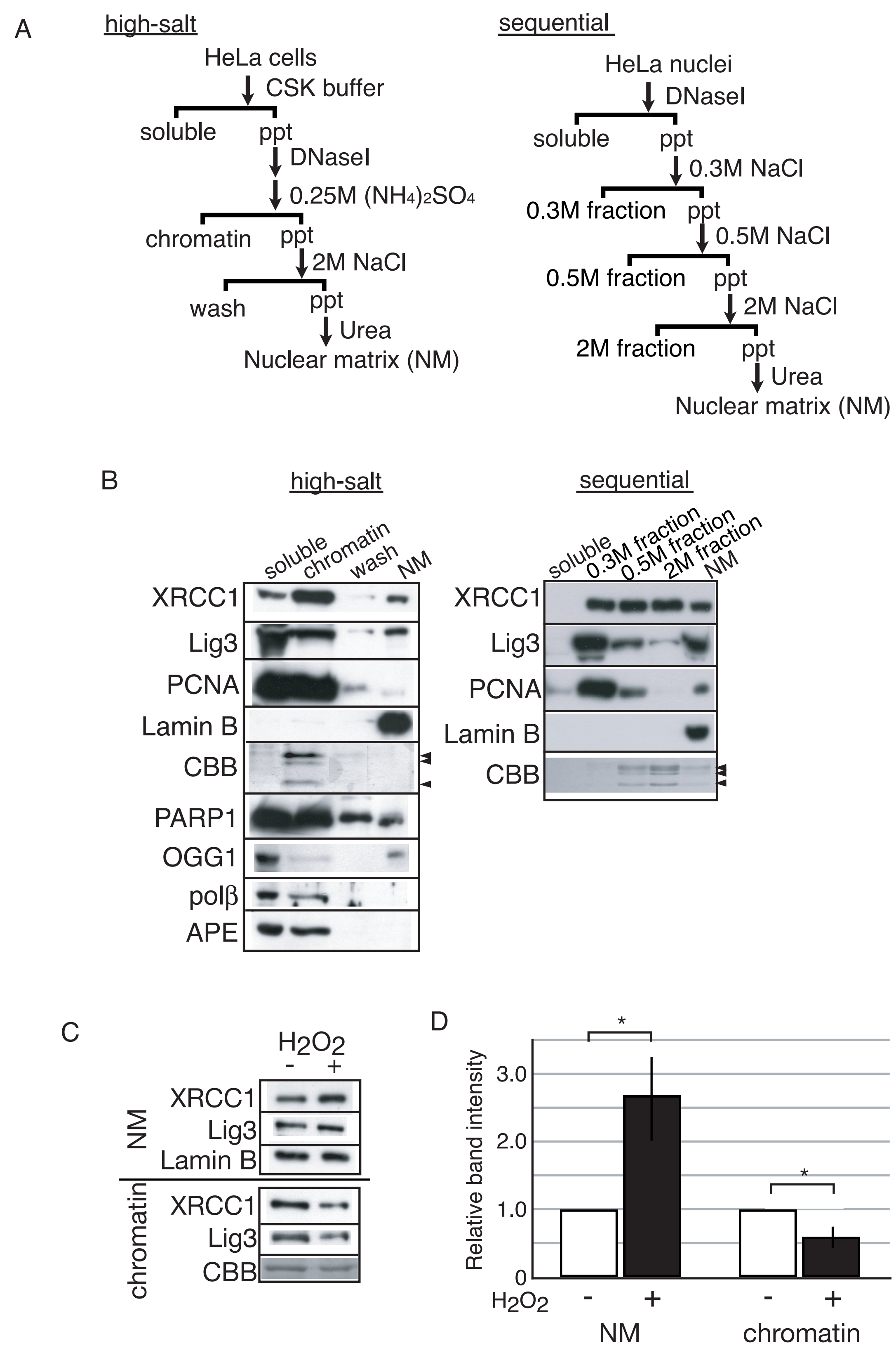
A
high-salt
HeLa cells
CSK buffer
soluble
ppt
DNaseI
0.25M (NH4)2SO4
chromatin
ppt
2M NaCl
wash
ppt
Urea
Nuclear matrix (NM)
sequential
HeLa nuclei
DNaseI
soluble
ppt
0.3M NaCl
0.3M fraction
ppt
0.5M NaCl
0.5M fraction
ppt
2M NaCl
2M fraction
ppt
Urea
Nuclear matrix (NM)
B
high-salt
soluble
chromatin
wash
NM
XRCC1
Lig3
PCNA
Lamin B
CBB
PARP1
OGG1
polβ
APE
sequential
soluble
0.3M fraction
0.5M fraction
2M fraction
NM
XRCC1
Lig3
PCNA
Lamin B
CBB
C
H2O2
-
+
NM
XRCC1
Lig3
Lamin B
chromatin
XRCC1
Lig3
CBB
D
Relative band intensity
3.0
2.0
1.0
0
*
*
H2O2
-
+
-
+
NM
chromatin

Figure 2

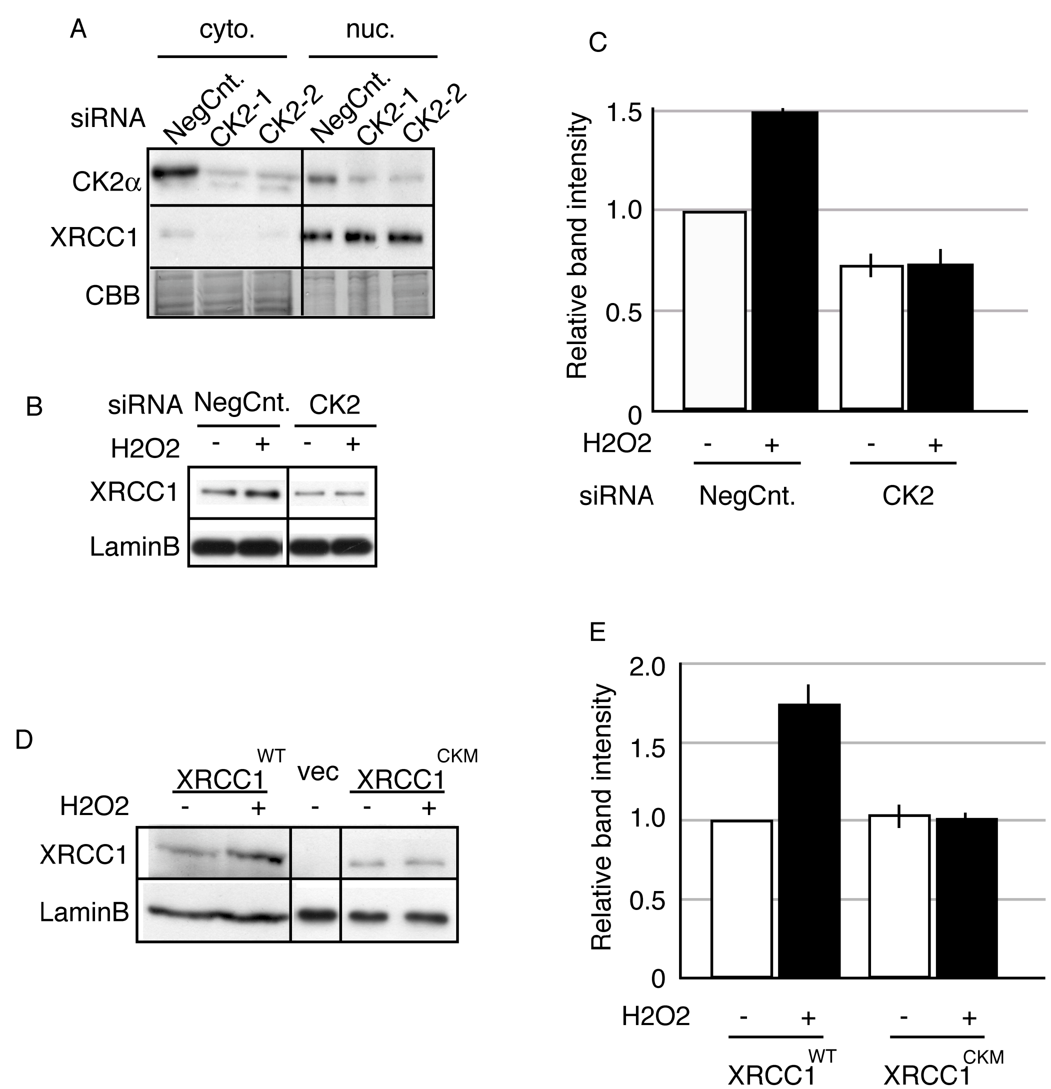

A
cyto.
nuc.
siRNA
NegCnt.
CK2-1
CK2-2
NegCnt.
CK2-1
CK2-2
CK2α
XRCC1
CBB
B
siRNA
NegCnt.
CK2
H2O2
- +
- +
XRCC1
LaminB
C
Relative band intensity
1.5
1.0
0.5
0
H2O2
- +
- +
siRNA
NegCnt.
CK2
D
XRCC1 WT
vec
XRCC1 CKM
H2O2
- +
-
- +
XRCC1
LaminB
E
Relative band intensity
2.0
1.5
1.0
0.5
0
H2O2
- +
- +
XRCC1 WT
XRCC1 CKM

Figure 3

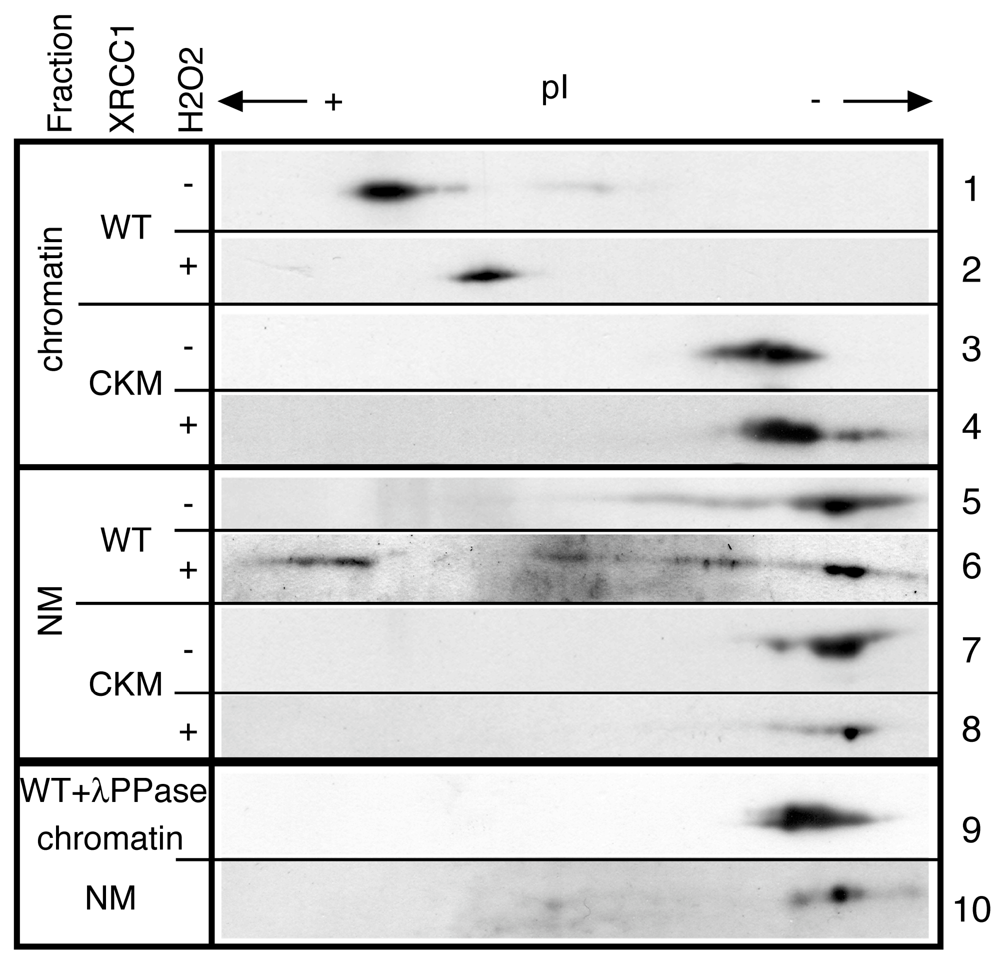

Fraction
XRCC1
H2O2
+
pI
-
chromatin
WT
CKM
NM
WT
CKM
WT+λPPase
chromatin
NM
-
+
-
+
-
+
-
+
1
2
3
4
5
6
7
8
9
10

Figure 4

A

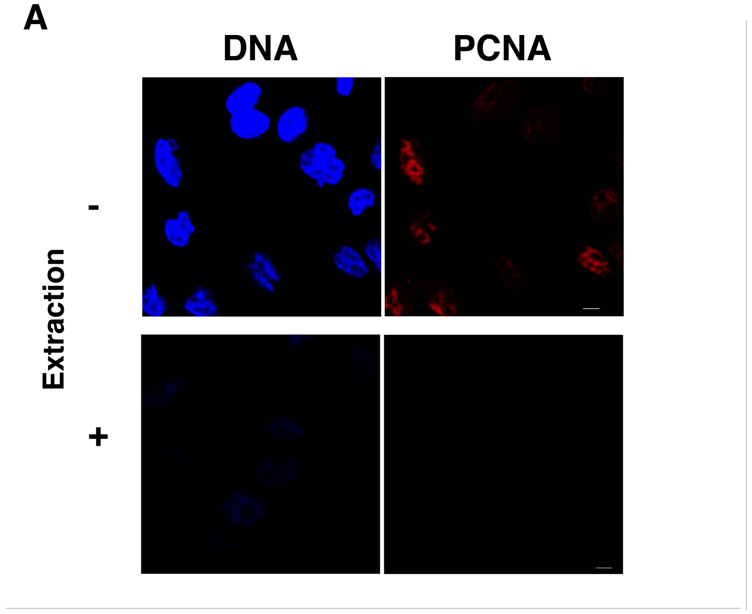

DNA
PCNA
Extraction
-
+

B

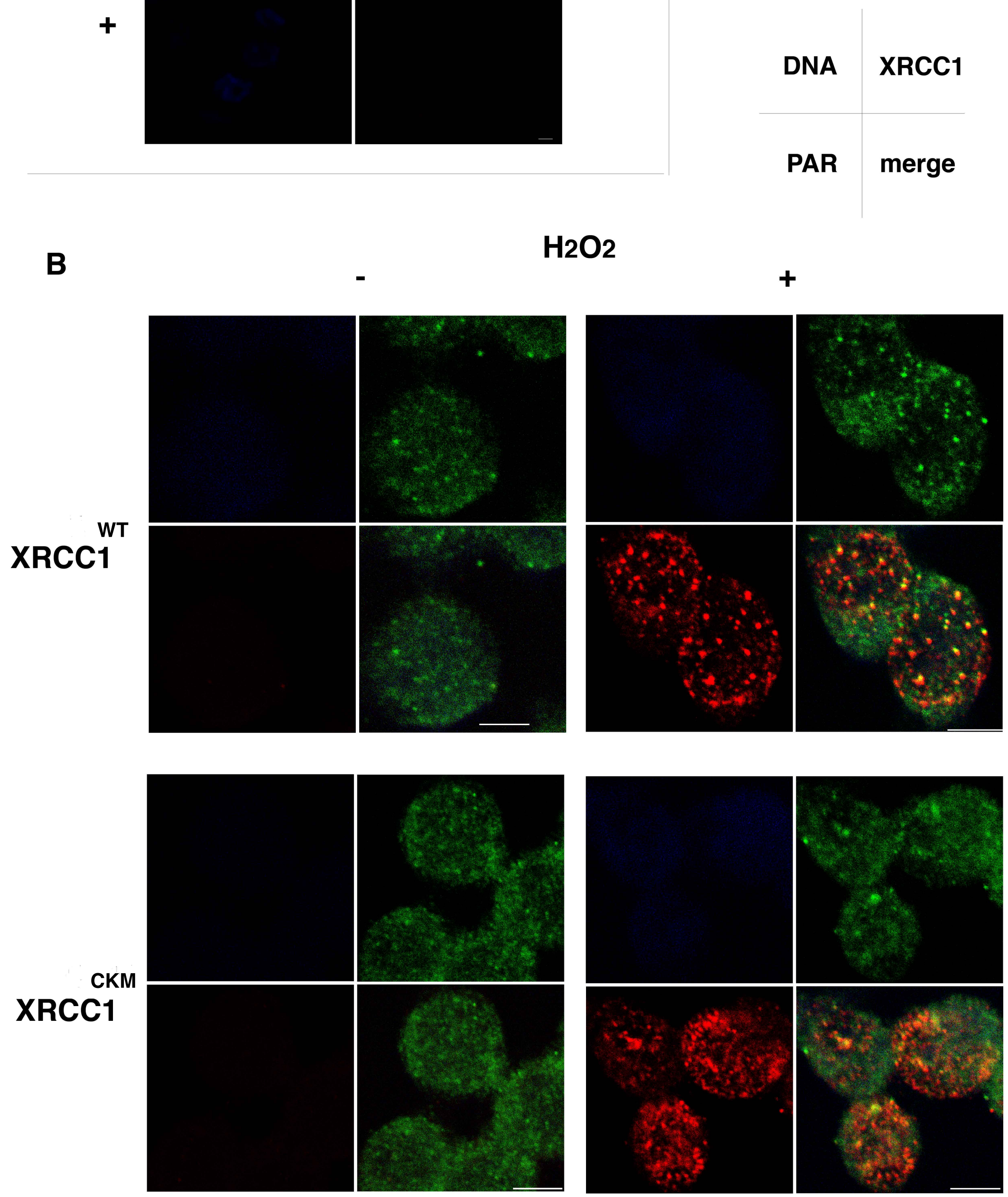

DNA
XRCC1
PAR
merge
H2O2
-
+
XRCC1 WT
XRCC1 CKM

Figure 5A

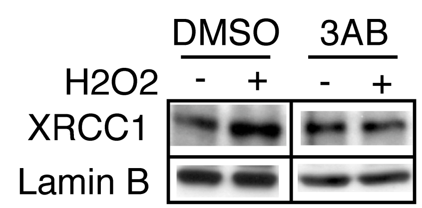

Figure 5B

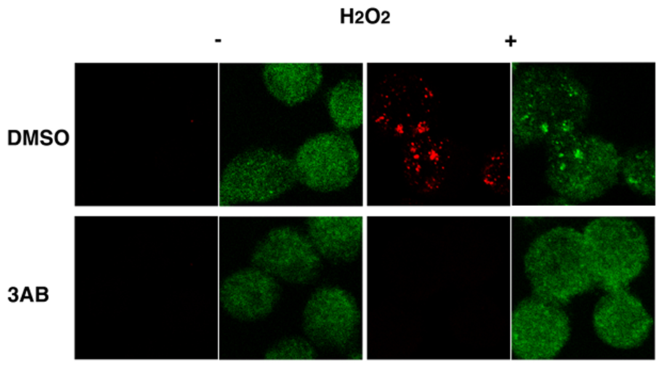

Figure 6